Annals of Botany **107**: 1501–1509, 2011
doi:10.1093/aob/mcr035, available online at www.aob.oxfordjournals.org

ANNALS OF BOTANY
Founded 1887

PART OF A SPECIAL ISSUE ON EVOLUTION AND DEVELOPMENT

Expression of floral identity genes in *Clianthus maximus* during mass inflorescence abortion and floral development

Jiancheng Song[1,2], John Clemens[1,2,3] and Paula E. Jameson[1,*]

[1]*School of Biological Sciences, University of Canterbury, Christchurch, New Zealand,* [2]*Institute of Molecular BioSciences, Massey University, Palmerston North, New Zealand and* [3]*Christchurch Botanic Gardens, Christchurch City Council, Christchurch, New Zealand*

** For correspondence. E-mail paula.jameson@canterbury.ac.nz*

Received: 31 August 2010 Returned for revision: 21 October 2010 Accepted: 4 January 2011 Published electronically: 7 March 2011

• *Background and Aims Clianthus maximus* is a leguminous perennial with an unusual order of floral organ insertion, and inflorescences produced year round that nearly all abort except during a limited time in autumn. This study aimed to determine at what point in floral organ differentiation abortion occurred and whether the expression of the floral identity genes underlies this cessation in flower development.
• *Methods* Inflorescences were harvested across an annual cycle and flower development was examined by light and scanning electron microscopy. Expression of the *C. maximus*-equivalents of *LEAFY* (*LFY*), *APETALA1* (*AP1*), *PISTILLATA* (*PI*) and *AGAMOUS* (*AG*) was monitored simultaneously by quantitative, reverse transcriptase PCR.
• *Key Results* Only those inflorescences formed in autumn proceeded to anthesis. Organogenesis had not begun in inflorescences that aborted. The *C. maximus*-equivalents of *AP1*, *PI* and *AG* were expressed in sepals, petals, carpels and stamens, as expected from the ABC model of floral organ identity specification; furthermore, the order of expression of the three genes reflected the unusual pattern of organ differentiation. Low expression of *LFY* and *AP1* was observed during inflorescence abortion.
• *Conclusions* Predictions of gene expression based on the ABC model were upheld despite the unusual mass abortion of inflorescences and the non-standard pattern of organ formation. The lack of expression of *LFY* and *AP1* in inflorescences may have been the cause of inflorescence abortion.

Key words: ABC model, *Clianthus maximus*, floral development, floral identity genes, gene expression, inflorescence abortion, *LEAFY*, *APETALA1*, *PISTILLATA*, *AGAMOUS*, qRT-PCR.

INTRODUCTION

Clianthus maximus (kowhai ngutukaka or kakabeak) is endemic to New Zealand and is listed as nationally vulnerable (de Lange *et al.*, 2004). It is a leguminous shrub and as such it is palatable to introduced deer and possums in its natural region, where it is found almost exclusively within 50 km of the east coast of the North Island of New Zealand. With its showy flowers it is also of outstanding horticultural value and is commonly cultivated. However, we have shown that the genetic diversity that remains in the wild is not retained in cultivation – and that which is in cultivation no longer exists in the wild (Song *et al.*, 2008*a*).

Despite its horticultural value and its endangered status, little is known of the floral ontogeny of *Clianthus* and details of flower development from inflorescence initiation to organ differentiation and development have not been published, nor has there been any expression analysis of the floral organ identity genes. The development of floral organs in the eudicots is widely accepted to be controlled by the combinatorial action of a set of homeotic genes – the Class A, Class B and Class C genes. Class A genes specify sepals, A and B combined specify petals, B and C combined specify stamens, and C genes alone specifies carpels (Bowman *et al.*, 1991; Coen and Meyerowitz, 1991). This designation of activities is commonly referred to as the ABC model of floral organ identity specification.

Quantitative reverse-transcriptase PCR (qRT-PCR) allows for the simultaneous analysis of multiple genes both during development and in specific organs. However, although the ABC model has been shown to be applicable to a wide range of species (Ng and Yanofsky, 2001; Becker and Theissen, 2003), simultaneous investigation of the expression of these genes during an entire annual cycle in natural conditions is limited to a few studies, including that of *Sophora tetraptera*, which is also a leguminous species native to New Zealand (Song *et al.*, 2008*b*).

We have reported contrasting programmes of floral development in *S. tetraptera* and *Metrosideros excelsa*, another woody species native to New Zealand. In *S. tetraptera*, inflorescence initiation started in late spring with all floral organs initiated by mid- to late summer. However, at this stage, development ceased and remained paused for several months. Then, in a rapid phase of development, floral organs were differentiated with full flowering occurring by October (Song *et al.*, 2008*b*).

In contrast, in *M. excelsa*, inflorescence development was only detectable by late autumn (May), and proceeded as far as cymule primordia in early winter (June) before a pause of several months through the winter. After this, organ differentiation proceeded rapidly with all floral organs fully

differentiating within 4–6 weeks by the end of September (Sreekantan *et al.*, 2001, 2004). We have shown (Henriod *et al.*, 2000) that several weeks of low temperatures are required during winter for cymules of *M. excelsa* to differentiate floral organs and not abort.

Here we show that the time frame of floral development in *C. maximus* differs from that of both *S. tetraptera* and *M. excelsa*. Inflorescences develop year-round, with only those inflorescences developing during a short period in late autumn proceeding to anthesis. A bimodal pattern of expression of *LEAFY* (*LFY*)- and *APETALA1* (*AP1*)-equivalents occurs in both *S. tetraptera* (Song *et al.*, 2008*b*) and *M. excelsa* (Sreekantan *et al.*, 2004), with a period of strong expression during initial inflorescence development, low expression of both genes during the winter 'pause' in floral development, followed by an increase during the spring flush of flower development. In this study, we used qRT-PCR to monitor the expression of the *Clianthus* equivalents of *LFY*, *AP1*, *PISTILLATA* (*PI*) and *AGAMOUS* (*AG*) during inflorescence and floral organ development, with the expectation that expression of the ABC genes in the individual floral organs of *Clianthus* would match the expression of the ABC genes in the floral organs of *Arabidopsis*, but that expression of the *LFY*- and *AP1*-equivalents might be reduced in those inflorescences destined to be aborted, with a consequent loss of the bimodal expression pattern exhibited by several woody species.

MATERIALS AND METHODS

Plant materials

Vegetatively propagated 3-year-old plants of *Clianthus maximus* 'Kaka King' were obtained from commercial nurseries and were grown in Palmerston North, New Zealand, under prevailing climatic conditions. Inflorescences and floral buds from different developmental stages were harvested at intervals of between 2 to 4 weeks (Supplementary Data Table S1, available online) from spring, over a complete annual growth cycle of vegetative and reproductive development. Monthly average temperature ranged from 15 to 20 °C in summer and from 5 to 10 °C in winter. For histological analysis, harvested samples were fixed initially in formalin–acetic acid–alcohol. Samples were then further prepared for light microscopy or scanning electron microscopy as detailed in Song *et al.* (2008*b*). For RNA isolation, harvested samples were frozen immediately in liquid nitrogen and stored at −80 °C until used.

Floral identity gene isolation and sequence analysis

Isolation of putative orthologues from *C. maximus* was carried out through direct sequencing of RT-PCR products using tissue-specific cDNA templates. For each gene of interest (GOI), degenerate primers were designed based on the sequence conservation of orthologues from *Arabidopsis thaliana*, *Antirrhinum majus*, all the legume sequences available in the NCBI database and 2–3 representative dicot species. For the MADS-box gene orthologues/paralogues, degenerate primers were designed to minimize the false isolation of any other coexisting paralogues or MADS-box genes from other subfamilies. Protein sequences were first aligned using the Clustal X program (Thompson *et al.*, 1997) to identify the conserved sequence segments. Corresponding DNA sequences of each conserved protein sequence segment were then aligned and degenerate primers were designed using Primer Premier 5·0 software. These primers were then searched against the NCBI database to verify their specificity; they are listed in Table 1.

TABLE 1. *Degenerate primers used for floral identity gene isolation from* Clianthus *(F, forward, R, reverse)*

Genes	Sequences (5′ to 3′)
LEAFY	F: CAAGGCTGCHRTHMGRGC
	R: GCTTKGTDGGNACRTACC
APETALA1	F: GGTAGRGTNCARYTGAAGMG
	R: GAGTCAGDTCVAGMTCRTTCC
PISTILLATA	F: GGMAAGATHGAGATMAAGMRG
	R: GCAGATTKGGCTCVAWNGG
AGAMOUS	F: GAGATHAAGMGVATHGARAAYAC
	R: CARMTCMAYYTCCCTYTTYTGC
β-Actin	F: GTGAAGGAAAAACATGCSTAYAT
	R: KGAACCACCACTCAAMACAATG
GAPDH	F: GACARTGGAARMACSAYGA
	R: TTCCACCTCTCCAGTCCTT
18S rRNA	F: TACCGTCCTAGTCTCAACCATAA
	R: AGAACATCTAAGGGCATCACA

Total RNA was extracted using a modification of the TRI reagent method (Molecular Research Centre, Cincinnati, OH, USA) as described in Song *et al.* (2008*b*). The quantity and purity of the RNA was measured using a NanoDrop ND-100 spectrophotometer (Nanodrop Technologies Inc., Wilmington, DE, USA). Its integrity was checked by visualization of ethidium-stained RNA separated on a 2 % (w/v) agarose gel containing 2 % formaldehyde. cDNA was synthesized using Expand Reverse Transcriptase (Roche Diagnostics, Mannheim, Germany) and used as a template for PCR as described in Song *et al.* (2008*b*). All bands of approximately the expected size were purified and sequenced on an ABS 3730 sequencer (Applied Bioscience) using the same degenerate primers as for the PCR. The raw sequences from four to eight sequencing reactions (at least two forward and two reverse directions) were aligned using Clustal X software to correct the sequencing errors and to generate a consensus sequence for each GOI.

For phylogenetic analysis, 13–20 representative orthologues/paralogues for each GOI (Supplementary Data Table S2) were used to construct both a neighbour-joining (NJ) phylogentic tree using Clustal X software and a maximum-likelihood (ML) tree using PhyML3·0 software (Guindon and Gascuel, 2003; Guindon *et al.*, 2010), with 1000 bootstrap replicates. Each tree was rooted with an orthologue/paralogue from the gymnosperm species *Pinus radiata.*

The nucleotide sequences reported in this paper were submitted to the GenBank database with the following accession numbers: *CmLFY*, DQ418756; *CmAP1*, DQ418757; *CmPI*, DQ418758; *CmAG*, DQ418759.

qRT-PCR

For qRT-PCR analysis, specific primers were designed for each gene as described in Song *et al.* (2008*b*) and are listed

in Supplementary Data Table S3. Primers were designed such that they were of similar size (within the range 100–350 nucleotides) and spanning at least one intron to eliminate amplification from genomic DNA. qRT-PCR analyses were performed using a LightCycler^{TM}2·0 and SYBR® Green DNA dye (Roche Diagnostics) as described in Song *et al.* (2008*b*).

To determine the PCR amplification efficiency of each GOI and housekeeping gene, a serial dilution of 10-, 100-, 1000-, 10 000- and 100 000-fold of the same cDNA was used for qRT-PCR amplification. A standard curve was obtained by plotting the threshold cycle (C_T) value versus the logarithm of the concentration. The PCR efficiency (E) was calculated according to the formula: $E = 10^{(-1/\text{slope})} - 1$ (Pfaffl, 2001).

Data analysis

As described in Song *et al.* (2008*b*), experimental data were analysed as a block experiment by analysis of variance, where PCR run was the block factor, the stage of development was the treatment factor and relative abundance was the response variable.

RESULTS

Floral ontogeny and development

Shoot growth (elongation and node number increase) and leaf emergence occurred continuously throughout the year. Vegetative growth slowed during the flowering season in early spring (September), and resumed in October after flowering. Inflorescences emerged from axils of undeveloped leaves within the shoot tip almost continuously throughout the year, from shortly after the previous flowering season in October until a short time before the next flowering season in August. The early-emerged inflorescences normally aborted during the development period. Furthermore, the inflorescences that emerged after May rarely reached the flowering stage and aborted before or during the flowering season. Only those inflorescences that emerged in autumn (April to early May) developed to maturity, with individual flowers developing to anthesis (Fig. 1). Inflorescences reached the flowering stage about 4 months after their emergence, with individual flower buds undergoing a series of developmental stages before opening in mid-September (Fig. 2O). There were 10–20 flowers in each inflorescence (Fig. 2P).

Microscopy studies confirmed that the inflorescences emerged from leaf axils (Fig. 2A) from November to August. Flower primordia were initiated within the inflorescence shortly thereafter (Fig. 2B). Although sepals could occasionally be distinguished between November and March, no further organogenesis was observed in flower primordia from inflorescences harvested before mid-April (Fig. 2C). Organogenesis progressed slowly from late April, with sepals (Fig. 2D) initiated first. This was followed by petal (Fig. 2E), outer stamen and carpel (Fig. 2F) initiation, which occurred sequentially but overlapped within a broadly similar time frame. The inner stamens initiated at the inner side of the petal primordia much later, when the mass of petals, outer stamens and carpel had increased substantially

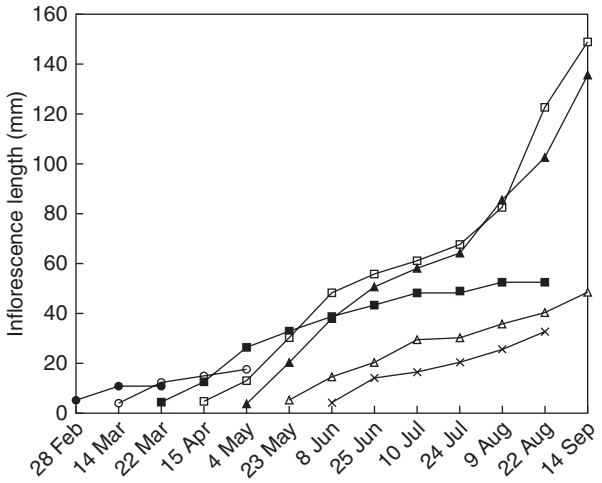

FIG. 1. Development of inflorescences of *C. maximus* emerging at different times of the year. Values are means of 25 inflorescences from five different plants. All inflorescences not elongating to >60 mm aborted.

(Fig. 2G). After all the organs within a floral bud had initiated, the floral organs enlarged and differentiated rapidly in June and early July. However, the increase in the mass of the carpel was substantially advanced over that of petals and outer stamens. The inner stamens remained much smaller than the floral organs in the other whorls (Fig. 2H–J). In late July, the size of the petals increased rapidly and further differentiated into distinct vexillum, wing and keel, with the height of the vexillum exceeding that of the carpel (Fig. 2K, L). At this stage, the height of the gynoecium still exceeded that of the androecium. By August, the volume of floral organs, particularly petals, had expanded further, with obvious formation of stigma, ovary and anthers. The androecium then enlarged so that its height now exceeded that of the gynoecium (Fig. 2M, N). At this time, the length of the flower bud was about 5–7 mm, equivalent to stage 1 of flower development (Fig. 2O).

Isolation of floral identity genes

Using the PCR product direct sequencing strategy, one single PCR product was obtained for each GOI. Results of multiple alignments of four to eight raw sequences confirmed that only one copy of each GOI was isolated from *C. maximus*. A single 401-bp putative *LFY* orthologue was obtained and was named *CmLFY*. All positive hits resulting from the BLAST search against the NCBI database were *LFY/FLO* orthologues from a large range of angiosperm and gymnosperm species. Multiple alignment of the deduced amino acid with related *LFY/FLO* orthologues showed that CmLFY has characteristics typical of a LFY and FLO orthologue and was most similar to the UNIFOLIATA (UNI) protein from the legume *Pisum sativum* (Supplementary Data Fig. S1, available online). Unexpectedly, the residue on position 20 of the CmLFY fragment differed from that of all other sequences, with the glutamic acid changed to aspartic acid. This is in agreement with our previous study in comparing the

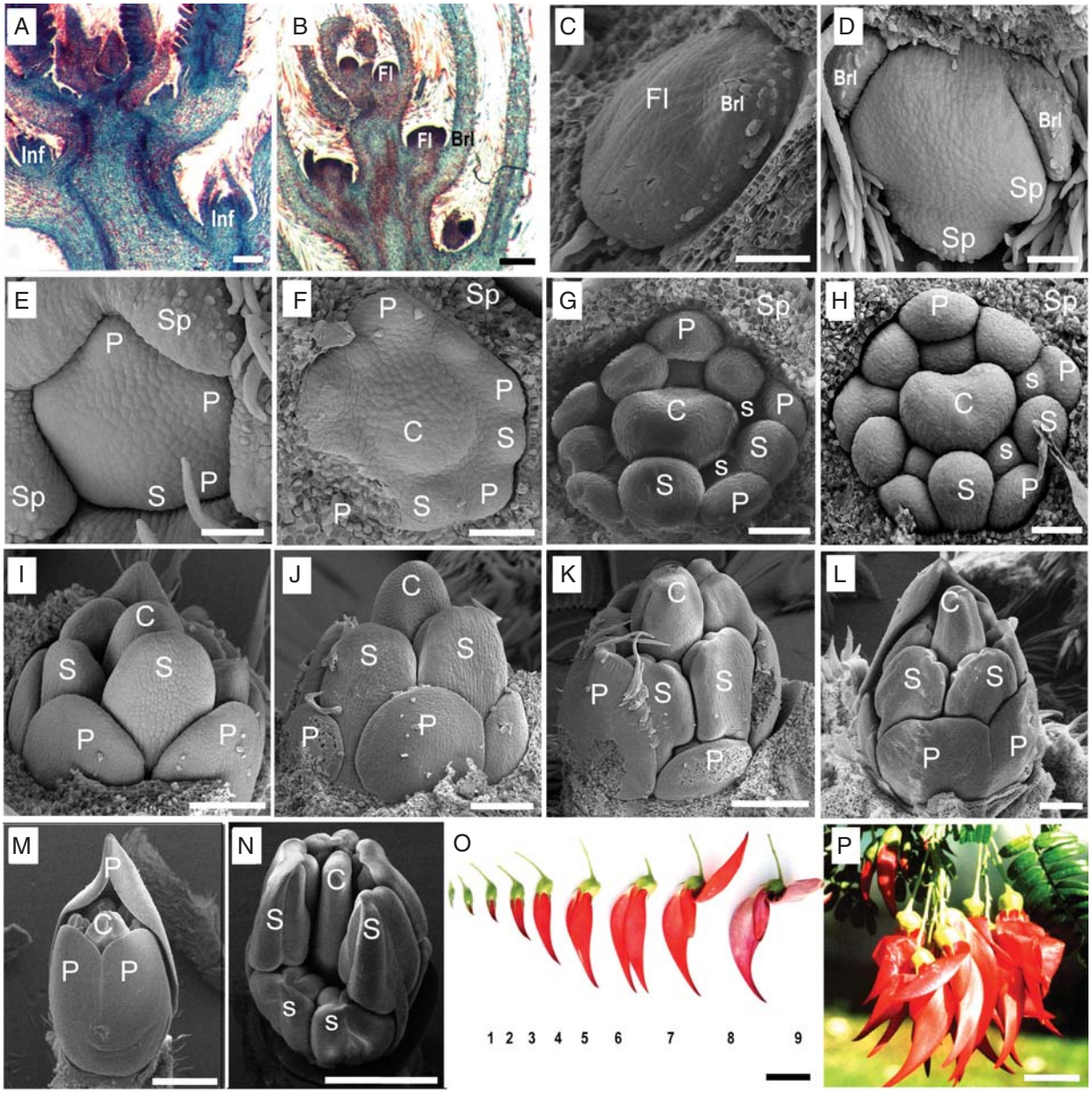

FIG. 2. Floral ontogeny and development in *C. maximus* using SEM (C–N) and light microscopy (A and B counter-stained with safranin and fast green). (A) Inflorescences initiated from the axil of the shoot tip; (B) inflorescence with floral primordia; (C) single floral meristem before organ initiation; (D) sepal initiation; (E) petal initiation; (F) outer stamen and carpel initiation; (G) mass increase of petals, outer stamens and carpel, with similar height; (H) inner stamen initiation; (I–K) organ differentiation and rapid enlargement; (L) petal expansion; (M) ovule formation; (N) pollen formation; (O) flower maturation; (P) inflorescences showing flowers in bloom. Abaxial side is at base of figure in (C–L). Sepals were removed in (F–L). Abbreviations: Brl, bracteole; C, carpel; Fl, flower buds; Inf, inflorescence; O, ovule; P, petal; S, outer stamen; s, inner stamen; Sp, sepal. Scale bars: (A, B, I, J) = 200 μm, (C–F) = 50 μm, (G, H) = 100 μm, (K, L) = 400 μm, (M, N) = 2 mm, (O, P) = 20 mm.

sequencing variability of *LEAFY* intron 2 for over 70 individual plants from cultivars and wild populations of the same species (Song *et al.*, 2008*b*). Similar tree topologies were obtained for the ML phylogenetic tree and the NJ phylogenetic tree using the same set of *LFY/FLO* orthologues, which showed that *CmLFY* grouped together with *LFY/FLO* orthologues of other eudicot species, and particularly with those of other leguminous species. It was well separated from the monocot *Zea mays* and the gymnosperm *Pinus radiata* (Fig. 3A, Supplementary Data Fig. S2).

The possible structure was deduced by comparison of the cDNA sequences and amino acid sequences with those of *Arabidopsis*. *CmLFY* spans the second intron, with 129 bp at the end of exon 1 and the rest of the sequence at the starting part of exon 3 (Supplementary Data Fig. S3).

The RT-PCR using degenerate *AP1* primers yielded a cDNA fragment of 629 bp. The fragment was named *CmAP1*. All of the sequences yielded by BLAST searching the GenBank amino acid database were AP1 and SQUA orthologue proteins. Multiple alignment of the deduced amino acid with related

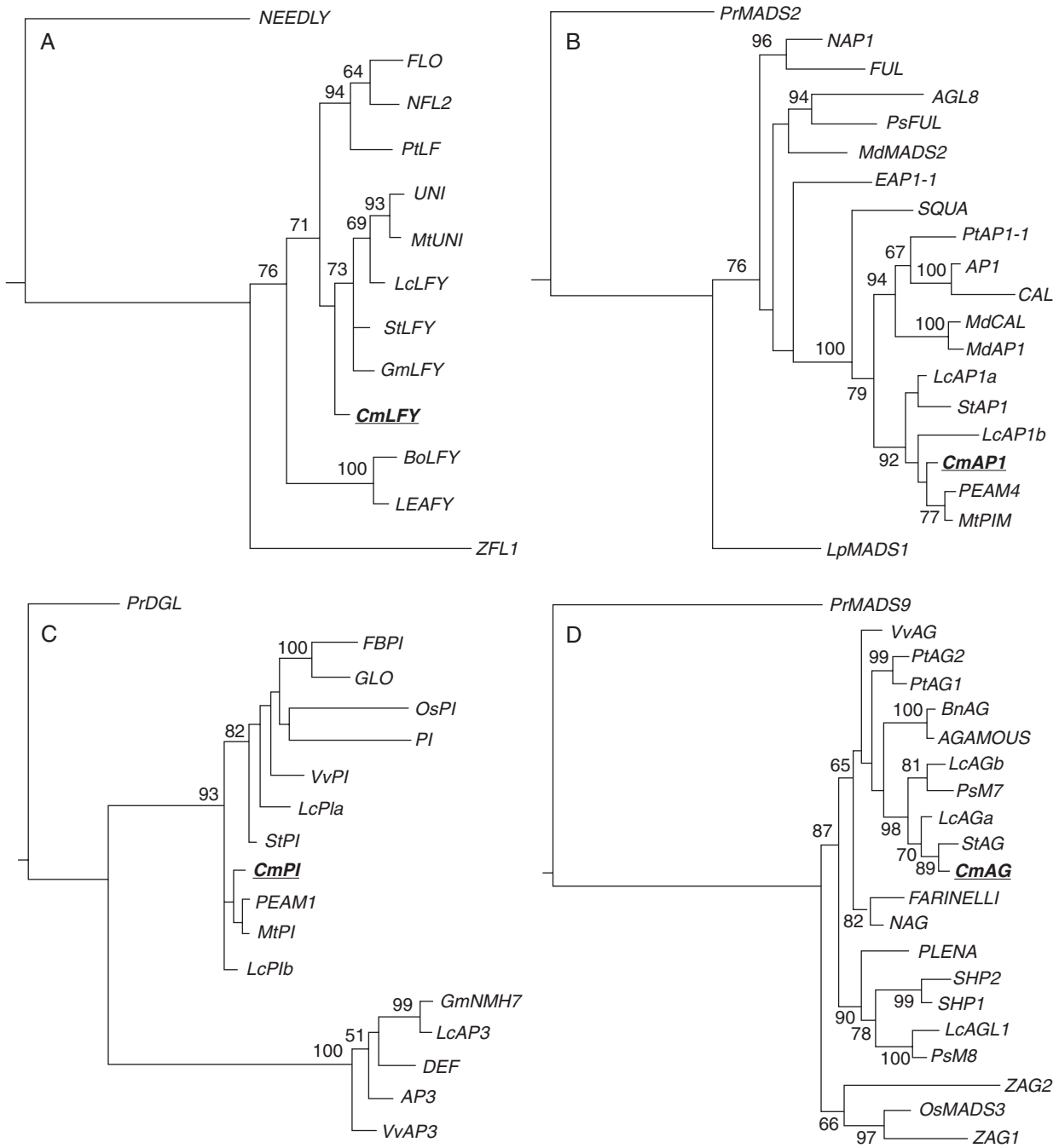

FIG. 3. The maximum-likelihood (ML) phylogentic trees of representative floral identity gene proteins generated with 1000 bootstrap replicates. Values are percentage bootstrap support. Genes isolated in this study are in bold font and are underlined. (A) *LFY*/*FLO* proteins. *BoLFY*, *Brassica oleracea*; *CmLFY*, *Clianthus maximus*, isolated in this study; *FLO*, *Antirrhinum majus*; *LFY*, *Arabidopsis thaliana*; *LcLFY*, *Lotus corniculatus* var. *japonicus*; *MtUNI*, *Medicago truncatula*; *NEEDLY*, *Pinus radiata*; *NFL2*, *Nicotiana tabacum*; *PtLF*, *Populus trichocarpa*; *StLFY*, *Sophora tetraptera*; *UNI*, *Pisum sativum*; *GmLFY*, *Glycine max*; *ZFL1*, *Zea mays*. Refer to Supplementary Data Table S2 (available online) for NCBI accession numbers. (B) Class A MADS-box proteins. *AGL8*, *AP1*, *CAL*, *Arabidopsis thaliana*; *CmAP1*, *Clianthus maximus*; *EAP1-1*, *Eucalyptus globulus*; *LcAP1a*, *b*, *Lotus corniculatus* var. *japonicus*; *LpMADS1*, *Lolium perenne*; *MdAP1*, *MdCAL*, *MdMADS2*, *Malus* × *domestica*; *MtPIM*, *Medicago truncatula*; *NAP1*, *Nicotiana tabacum*; *PEAM4*, *PsFUL*, *Pisum sativum*; *PrMADS2*, *Pinus radiata*; *PtAP1-1*, *Populus trichocarpa*; *FRUITFUL*, *SQUA*, *Antirrhinum majus*; *StAP1*, *Sophora tetraptera.* Refer to Supplementary Data Table S2 for NCBI accession numbers. (C) Class B MADS-box proteins. *AP3*, *PI*, *Arabidopsis thaliana*; *CmPI*, *Clianthus maximus*; *DEF*, *GLO*, *Antirrhinum majus*; *FBPI*, *Petunia hybrida*; *GmNMH7*, *Glycine max*; *LcPIa*, *b*, *LcAP3*, *Lotus corniculatus* var. *japonicus*; *MtPI*, *Medicago truncatula*; *OsPI*, *Oryza sativa*; *PEAM1*, *Pisum sativum*; *PrDGL*, *Pinus radiata*; *StPI*, *Sophora tetraptera*; *VvAP3*, *VvPI*, *Vitis vinifera*. Refer to Supplementary Data Table S2 for NCBI accession numbers. (D) Class C MADS-box proteins. *AG*, *SHP1*, *SHP2*, *Arabidopsis thaliana*; *BnAG*, *Brassica napus*; *CmAG*, *Clianthus maximus*; *FARINELLI*, *PLE*, *Antirrhinum majus*; *LcAGa*, *LcAGb*, *LcAGL1*, *Lotus corniculatus* var. *japonicus*; *NAG1*, *Nicotiana tabacum*; *OsMADS3*, *Oryza sativa*; *PsM7*, *PsM8*, *Pisum sativum*; *PtAG1*, *PtAG2*, *Populus trichocarpa*; *PrMADS9*, *Pinus radiata*; *StAG*, *Sophora tetraptera*; *VvAG*, *Vitis vinifera*; *ZAG1*, *ZAG2*, *Zea mays*. Refer to Supplementary Data Table S2 for NCBI accession numbers.

Class A MADS-box proteins showed that CmAP1 has characteristics typical of an AP1 orthologue and the most similar protein was PEAM4 from the legume *Pisum sativum* (Supplementary Data Fig. S4). To elucidate the relationship of CmAP1 with other orthologues in a broad taxonomic range, 20 Class A MADS-box proteins from eudicot and one monocot species were compared to generate phylogenetic trees. Both the ML and the NJ phylogenetic trees clearly showed the eudicot AP1/SQUA orthologues grouped together and well separated from the monocot species. CmAP1 showed closest relationship to other leguminous species (Fig. 3B, Supplementary Data Fig. S5). In comparing the cDNA and amino acid sequences, the segment sequenced covered exons 1–8, including the major part of the MADS-box, and the entire sequence of the K-domain (Supplementary Data Figs S3 and S5).

A 329-bp putative *PI* orthologue for *Clianthus* was obtained through RT-PCR and direct sequencing and was named *CmPI*. BLAST searches for similar sequences in the GenBank amino acid database with CmPI yielded only PI/GLO sequences. Multiple alignment of the deduced amino acid with related Class B MADS-box proteins showed that CmPI has characteristics typical of a PI/GLO orthologue and the most similar protein was PEAM1 from the legume *Pisum sativum* (Supplementary Data Fig. S6). Phylogenetic trees generated using 15 Class B MADS-box gene proteins were compared to determine the relationship of CmPI with orthologues/paralogues in other species. Both rooted NJ and ML trees showed that CmPI was grouped most closely to the other leguminous species of the PI/GLO clade and was well separated from those of the AP3/DEF clade (Fig. 3C, Supplementary Data Fig. S7). The *CmPI* fragment consisted of the entire sequences for exons 1–3 and the partial sequence of exon 4 and covered the entire MADS-box and partial sequence of the K-domain (Supplementary Data Figs S3 and S6).

Similarly, a 297-bp putative *AG* orthologue was isolated and named *CmAG*. All of the sequences found by BLAST searches of the CmAG amino acid sequence against the GenBank amino acid database were AG/PLE orthologue proteins. Multiple alignment of the deduced amino acid with related Class C MADS-box proteins showed that CmAG has characteristics typical of an AG orthologue and the most similar protein was LcAGa from the legume *Lotus corniculatus* var. *japonicus* (Supplementary Data Fig. S8). The rooted ML and NJ phylogenetic trees of the representative Class C MADS-box proteins showed that CmAG clustered with other leguminous species, and that it was more closely related to the AG/FAR orthologues than the PLE/SHP orthologues (Fig. 3D, Supplementary Data Fig. S9). The CmAG fragment consisted of exons 2–5 and contained a short sequence of the MADS-box and almost the entirety of the K-domain (Supplementary Data Figs S3 and S8).

Housekeeping genes and qRT-PCR optimization

Orthologues of housekeeping genes *18S*, *β-actin* and *GAPDH* from *Clianthus* were isolated using the same strategy as for the GOIs and were used as internal controls in the gene expression studies. Optimization of the qRT-PCR is described in detail in Song *et al.* (2008*b*). The PCR efficiencies are shown in Table 2 for both floral identity genes and housekeeping genes.

TABLE 2. *PCR efficiencies of floral identity genes and selected housekeeping genes*

Gene	Slope	Efficiency
CmAP1	−3·646	0·881
CmPI	−3·540	0·916
CmAG	−3·497	0·932
CmLFY	−3·662	0·875
Cm18S	−3·389	0·973
CmGAPDH	−3·663	0·875
CmACT	−3·566	0·907

PCR efficiencies were calculated according to the formula: Efficiency = $10^{(-1/\text{slope})} - 1$ (Pfaffl, 2001). The slope was calculated based on the standard curve generated using a serial dilution of 10-, 100-, 1000-, 10 000- and 100 000-fold of the same cDNA template.

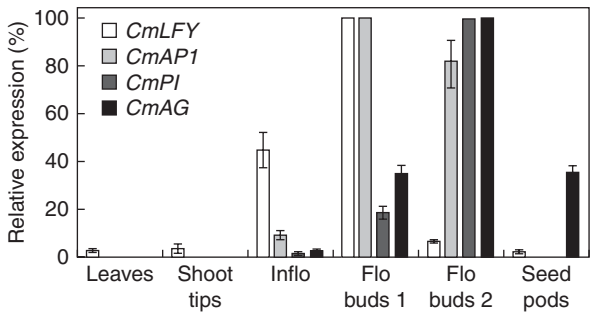

FIG. 4. Expression of floral identity genes in selected vegetative and reproductive tissues of *C. maximus*. Relative mRNA levels were determined using qRT-PCR and normalized using housekeeping genes *18S*, *GAPDH* and *β-actin* as internal controls. Values are mean ± s.e. of four replicates. Inflo, inflorescences 2–3 mm in length; Flo Bud 1, early-stage flower buds 2–3 mm in length; Flo Bud 2, mid-stage flower buds 18–20 mm in length; Seed pods, 2–3 weeks after flowering.

Expression of floral identity genes in vegetative and reproductive tissues

Expression of the four floral identity genes was analysed in shoot tips, adult leaves and inflorescences harvested in late autumn (May), and from early-stage flower buds, mid-stage flower buds and seed pods sampled in July, September and October, respectively. A distinct expression profile was obtained for each gene (Fig. 4). Relative to the expression of *CmLFY* in early-stage flower buds (set at 100 %), expression decreased to 7 % in mid-stage flower buds. Expression was low in leaves and vegetative shoot tips (2–3 %) and was barely detectable in seed pods (1·7 %). *CmLFY* expressed at relatively high levels in inflorescences (45 %).

No *CmAP1* activity was detected in adult leaves, vegetative shoot tips or seed pods. The highest level of expression was in early-stage flower buds (100 %) and in mid-stage flower buds (82 %), but a relatively low level (9 %) was detected in inflorescences.

CmPI expression was not detected in leaves, vegetative shoot tips or seed pods. Inflorescences and early-stage flower

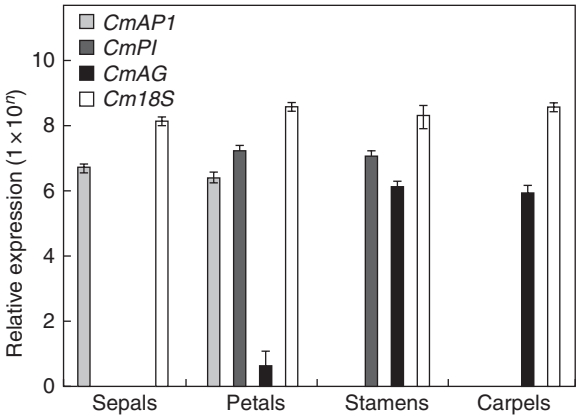

FIG. 5. Expression of floral organ identity genes and the *18S* orthologue in different floral organs of *C. maximus*. Ten flower buds at late developmental stage (18–20 mm in length showing petal tip) were individually dissected to obtain a mixed sample of each floral organ. Relative mRNA levels were determined using qRT-PCR, calculated and presented on a logarithmic scale across all the tested genes. Values are mean ± s.e. of three replicates.

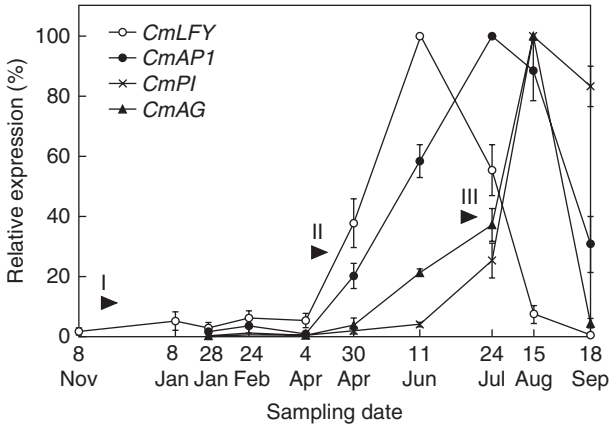

FIG. 6. Expression profiles of floral identity genes in *C. maximus* during a complete growth cycle. Relative mRNA levels were determined using qRT-PCR and normalized using housekeeping genes *18S*, *GAPDH* and *β-actin* as internal controls. Values are mean ± s.e. of four replicates. Arrows show the starting points of: I, floral meristem initiation; II, floral organ initiation; III, floral organ differentiation and development. Sample descriptions: 8 Nov to 8 Jan, shoot tips with/without inflorescence primordia; 28 Jan to 30 Apr, inflorescences (15–20 mm) with floral primordia; 11 Jun, inflorescences (25–35 mm) with flower bud (approx. 1 mm) and all floral organs initiated; 24 Jul, flower buds (2–3 mm) with well-differentiated floral organs and elongated anthers and pistils; 15 Aug, flower buds (10–12 mm) showing petal tip, with well-formed pollen and ovules; 18 Sep, mature flower buds before opening.

buds had low levels of expression (19 and 1·5 %, respectively) relative to high expression in mid-stage flower buds (100 %).

The highest *CmAG* expression was detected in mid-stage flower buds, whereas expression was low in inflorescences (2·4 %) and early-stage flower buds (35 %). No *CmAG* expression was detected in adult leaves and vegetative shoot tips but significant (35 %) *CmAG* expression was detected in seed pods.

Organ-specific expression of floral organ identity genes

Sepals, petals, stamens and carpels were excised from flower buds in early spring (September) when the flower buds were beginning to show the tips of petals (Fig. 2O, Stage 2). Expression of *CmAP1*, *CmPI* and *CmAG* was assessed using *Cm18S* as an internal control (Fig. 5). *CmAP1* expression was found only in sepals and petals, *CmPI* expression was detected in petals and stamens, but not in sepals or carpels, and *CmAG* expression occurred at high levels in stamens and carpels but was also detected in petals at a low level (albeit 1000-fold lower than in the other organs).

Expression profiles of floral organ identity genes during a growth cycle

Given that the floral identity genes showed differential expression during different stages of flower development, and given that there is a continuous cycle of inflorescence formation and abortion up until those formed in May which develop through to flowering, a detailed expression profile of the genes was obtained across a developmental cycle (Fig. 6). In this cycle, shoot tips were harvested from November, inflorescences were harvested from January to April, and from June to September samples were of flower buds.

In shoot tips, *CmLFY* expression remained at a very low level from August to April (2–5 %) compared with its highest expression in June. In inflorescences and floral buds, expression of the four GOIs was low from January to early April. Increasing levels of these genes were detected from April to September but this occurred in a sequential manner: *CmLFY* peaked in June, *CmAP1* in July, and *CmPI* and *CmAG* in September. *CmPI* expression remained high (>80 %) during flowering in September whereas that of the other genes had declined by that time.

DISCUSSION

Floral development in *Clianthus* follows an unusual pattern with significant resource being allocated to inflorescence development throughout much of the year, only for the bulk of those inflorescences to be aborted. Only those inflorescences formed during a few weeks in autumn proceed to maturity. Light and scanning electron microscopy of *Clianthus* established that organogenesis had not begun in the inflorescences destined to be aborted. The pattern of organogenesis, once begun, essentially followed the order detailed for the model plants of sepals, petals, stamens and carpel. However, the inner stamen whorl was not established until after the carpel was initiated and the carpel primodium had enlarged. The carpel was also much more advanced than that of the floral organs in whorls 2 and 3, and its height was superior to that of the other organs until the formation of the gametocytes. In addition, there was a significantly delayed expansion of the petals.

Genes controlling the specification of floral organ identity and development have been isolated and characterized in a variety of plant species. Intensive studies and analysis of homeotic mutants in *Arabidopsis* and *Antirrhinum* led to the ABC model of floral organ identity specification (Bowman *et al.*, 1991; Coen and Meyerowitz, 1991; Weigel *et al.*, 1992).

Analyses have largely substantiated the applicability of this model, but simultaneous and quantitative expression of A, B, and C orthologues has rarely been carried out in plants across an entire life cycle (e.g. Song *et al.*, 2008*b* in *Sophora*). This is of particular interest in species that show unusual floral development, such as the mass abortion of inflorescences exhibited by *Clianthus*, and different patterns of organogenesis, as in the papilionoid legumes (Tucker, 2003).

To further establish the genetic control of inflorescence and floral development, the *Clianthus* equivalents of *LFY*, *AP1*, *PI* and *AG* were isolated. The combined information from the BLAST searches against the GenBank database, the multiple sequence alignments, the phylogenetic trees aligning the sequences into the expected taxonomic relationships and the gene structures all suggest that we have isolated from *Clianthus* the gene orthologues of *LFY/FLO*, *AP1/SQUA*, *PI/GLO* and *AG/FARINELLI* or *SHP/PLE* from *Arabidopsis* and *Antirrhinum*, respectively. qRT-PCR then enabled us to monitor simultaneously the expression of these genes during inflorescence development and abortion, and flower development. The high sequence similarity lends support to the hypothesis that the ABC model would be broadly applicable to *Clianthus*. Optimization of the qRT-PCR approach used has been described previously (Song *et al.*, 2008*b*).

Expression of *CmAP1*, *CmPI* and *CmAG* agreed with that predicted by the ABC model: as expected, the Class A gene *CmAP1* was expressed in the sepals and petals; the Class B gene *CmPI* was expressed in petals and stamens; and the Class C gene *CmAG* was expressed in stamens and carpels. The additional expression of *CmAG* in seed pods was not unexpected as this was also found in *S. tetraptera* (Song *et al.*, 2008*b*).

In those *C. maximus* inflorescences that did not abort but proceeded through to flowering, changes in the levels of the four GOIs did not track in the order of the model plant *Arabidopsis* (i.e. A then AB, BC and then C), but reflected the developmental sequence as shown by scanning electron microscopy. Sepals appeared first as did the increase in the Class A gene, *CmAP1*. However, the Class C gene, *CmAG*, then increased reflecting the strong development of the carpel. Subsequently, *CmPI* increased and both genes peaked simultaneously, along with *CmAP1* expression, possibly reflecting a requirement for expression of all three homeotic genes throughout organ development. *S. tetraptera*, which also exhibits an unusual sequence of floral organ development, showed a similar altered pattern of gene expression (Song *et al.*, 2008*b*).

While the alignment of the floral identity genes is as predicted, the abortion of inflorescences is an unusual phenomenon. In a number of woody species with prolonged patterns of floral development, and in which expression of *LFY* and/or *AP1* has been monitored, a bimodal pattern of expression has been observed with expression of *LFY* and/or *AP1* elevated at the initial stages of floral development followed by a decrease, usually through a winter dormancy period, after which expression of these genes again increased. Such a bimodal pattern of expression was first shown, by northern blot analysis, for both *LFY*- and *AP1*-equivalents, in *Actinidia deliciosa* (Walton *et al.*, 2001). A similar bimodal pattern was shown for the *LFY*-equivalent of *Vitis* (Carmona *et al.*, 2002). In *M. excelsa* flowers, which develop in one season, the temporal expression patterns showed both *LFY*- and *AP1*-equivalents to be elevated during early floral initiation in autumn, down-regulated during winter and up-regulated during floral organ differentiation in spring. In contrast to the above winter-dormant species, *S. tetraptera* exhibits a summer–autumn dormancy during floral development but here, again, a definitive bimodal pattern of expression occurs: peaks of expression of *StLFY* and *StAP1* coincided with floral organ initiation and subsequently with floral organ differentiation, as shown by Song *et al.* (2008*b*) using qRT-PCR.

In *C. maximus*, at the transition from the vegetative to the reproductive phase with the formation of the inflorescence, we might have expected enhanced activity of *CmLFY* and/or *CmAP1* as occurred in the woody species mentioned above. However, throughout the months when inflorescences were being formed and aborted, little activity of *CmLFY* was detected and no expression of *CmAP1*. Both *LFY* and *AP1* are considered necessary for floral meristem initiation (Liu *et al.*, 2009), and Kaufmann *et al.* (2010) suggest that *AP1* acts to down-regulate floral repressors during the earliest stages of flower development. It is clear from our work that expression of both *CmLFY* and *CmAP1* is essentially lacking in *Clianthus* plants until late autumn (May). The sequence of events that occurs at this time that lead to the up-regulation of *CmLFY* and *CmAP1* is yet to be determined.

In conclusion, predictions of gene expression based on the ABC model were upheld despite the unusual mass abortion of inflorescences and the non-standard pattern of organ formation. We suggest that the lack of expression of *LFY* and *AP1* in inflorescences may have been the cause of inflorescence abortion.

SUPPLEMENTARY DATA

Supplementary data are available online at www.aob.oxfordjournals.org and consist of the following tables and figures. Table S1: Tissue samples of *Clianthus maximus* ‘Kaka King’ for RNA isolation. Table S2: Floral identity gene homologues used for multiple alignment and phylogenetic analysis. Table S3: qRT-PCR primers for expression analysis of floral identity genes and housekeeping genes in *Clianthus*. Fig. S1: Comparison of amino acid sequences of CmLFY with representative FLO/LFY-like proteins. Fig. S2: Neighbour-joining phylogenetic tree of representative FLO/LFY orthologues. Fig. S3: Deduced gene structure of *CmLFY*, *CmAP1*, *CmPI* and *CmAG* fragments in *C. maximus*. Fig. S4: Comparison of amino acid sequences of CmAP1 with representative Class A MADS-box gene proteins. Fig. S5: Neighbour-joining phylogenetic tree of representative Class A MADS-box gene proteins. Fig. S6: Comparison of amino acid sequences of CmPI with representative Class B MADS-box gene proteins. Fig. S7: Neighbour-joining phylogenetic tree of representative Class B MADS-box gene proteins. Fig. S8: Comparison of amino acid sequences of CmAG with representative Class C MADS-box gene proteins. Fig. S9: Neighbour-joining phylogenetic tree of representative Class C MADS-box gene proteins.

ACKNOWLEDGEMENTS

This work was supported by the New Zealand Foundation for Research, Science & Technology Public Good Science Fund under the Native Ornamental Plants Programme through subcontract C02X0015 to Crop & Food Research and a Massey PhD scholarship (J.S.). We acknowledge Mr Neil Andrew for his technical assistance (SEM).

LITERATURE CITED

Becker A, Theissen G. 2003. The major clades of MADS-box genes and their role in the development and evolution of flowering plants. *Molecular Phylogenetics and Evolution* **29**: 464–489.

Bowman JL, Smyth DR, Meyerowitz EM. 1991. Genetic interactions among floral homeotic genes of Arabidopsis. *Development* **112**: 1–20.

Carmona MJ, Cubas P, Martinez-Zapater JM. 2002. *VFL*, the grapevine *FLORICAULA/LEAFY* ortholog, is expressed in meristematic regions independently of their fate. *Plant Physiology* **130**: 68–77.

Coen ES, Meyerowitz EM. 1991. The war of the whorls: genetic interactions controlling flower development. *Nature* **353**: 31–37.

Guindon S, Gascuel O. 2003. A simple, fast and accurate algorithm to estimate large phylogenies by maximum likelihood. *Systematic Biology* **52**: 696–704.

Guindon S, Dufayard JF, Lefort V, *et al*. 2010. New algorithms and methods to estimate maximum-likelihood phylogenies: assessing the performance of PhyML 3·0. *Systematic Biology* **59**: 307–321.

Henriod RE, Jameson PE, Clemens J. 2000. Effects of photoperiod, temperature and bud size on flowering in *Metrosideros excelsa* (Myrtaceae). *Journal of Horticultural Science and Biotechnology* **75**: 55–61.

Kaufmann K, Wellmer F, Muiño JM, *et al*. 2010. Orchestration of floral initiation by *APETALA1*. *Science* **328**: 85–89.

de Lange PJ, Norton DA, Heenan PB, *et al*. 2004. Threatened and uncommon plants of New Zealand. *New Zealand Journal of Botany* **42**: 45–76.

Liu C, Thong Z, Yu H. 2009. Coming into bloom: the specification of floral meristems. *Development* **136**: 3379–3391.

Ng M, Yanofsky MF. 2001. Function and evolution of the plant MADS-box gene family. *Nature Reviews Genetics* **2**: 186–195.

Pfaffl MW. 2001. A new mathematical model for relative quantification in real-time RT-PCR. *Nucleic Acids Research* **29**: e45. doi:10.1093/nar/29.9.e45

Song J, Murdoch J, Gardiner SE, Young A, Jameson PE, Clemens J. 2008*a*. Molecular markers and a sequence deletion in intron 2 of the putative partial homologue of *LEAFY* reveal geographical structure to genetic diversity in the acutely threatened legume genus *Clianthus*. *Biological Conservation* **141**: 2041–2053.

Song J, Clemens J, Jameson PE. 2008*b*. Quantitative expression analysis of the ABC genes in *Sophora tetraptera*, a woody legume with an unusual sequence of floral organ development. *Journal of Experimental Botany* **59**: 247–259.

Sreekantan L, McKenzie MJ, Jameson PE, Clemens J. 2001. Cycles of floral and vegetative development in *Metrosideros excelsa* (Myrtaceae). *International Journal of Plant Sciences* **162**: 719–727.

Sreekantan L, Clemens J, McKenzie MJ, Lenton JR, Croker SJ, Jameson PE. 2004. Flowering genes in *Metrosideros* fit a broad herbaceous model encompassing *Arabidopsis* and *Antirrhinum*. *Physiologia Plantarum* **121**: 163–173.

Thompson JD, Gibson TJ, Plewniak F, Jeanmougin F, Higgins DG. 1997. The Clustal_X windows interface: flexible strategies for multiple sequence alignment aided by quality analysis tools. *Nucleic Acids Research* **25**: 4876–4882.

Tucker SC. 2003. Floral development in legumes. *Plant Physiology* **131**: 911–926.

Walton EF, Podivinsky E, Wu RM. 2001. Bimodal patterns of floral gene expression over the two seasons that kiwifruit flowers develop. *Physiologia Plantarum* **111**: 396–404.

Weigel D, Alvarez J, Smyth DR, Yanofsky MF, Meyerowitz EM. 1992. *LEAFY* controls floral meristem identity in Arabidopsis. *Cell* **69**: 843–859.